Three component, three dimensional X-ray particle image velocimetry using multiple projections

Stephen Dubsky[1,2,5], Andreas Fouras [1,2,6], Sarah C. Irvine[3,7], Karen K.W. Siu[3,8], Kerry Hourigan[1,2,9]

1: Division of Biological Engineering, Monash University, Melbourne, Australia
2: Fluids Laboratory for Aeronautical and Industrial Research (FLAIR), Dept. Mechanical Engineering, Monash University, Melbourne, Australia
3: School of Physics, Monash University, Melbourne, Australia
4: Monash Centre for Synchrotron Science, Monash University, Melbourne, Australia
5: Stephen.Dubsky@eng.monash.edu.au
6: Fouras@eng.monash.edu.
7: Sally.Irvine@sci.monash.edu.au
8: Karen.Siu@sync.monash.edu.au
9: Kerry.Hourigan@eng.monash.edu.au

Abstract An X-ray PIV technique is described which provides three components of velocity measurement in three dimensional space. Current X-ray PIV techniques, which use particle images taken at a single projection angle, are limited to two components of velocity measurement, and are unable to measure in three dimensions without *a priori* knowledge of the flow field. The proposed method uses multiple projection angles to overcome these limitations. The velocity field is reconstructed in axial slices, defined by the rows of the interrogation regions. A three component, two dimensional, bicubic spline model represents the velocity profile for each slice. The velocity coefficients are optimised using a non-linear iterative scheme, minimising the error between measured cross correlation functions calculated from the image pairs and those estimated using the flow model. The minimisation is performed across all projection angles and interrogation regions simultaneously, resulting in a flow model which accurately represents the velocity field within each slice. The technique is tested using synthetic data sets and is found to perform well for both axisymmetric and asymmetric flows, with as few as 13 projection angles. The proposed method, which provides the capability to measure complex three dimensional, three component velocity fields in opaque vessels, represents a significant advancement in X-ray PIV, with applications in the diagnosis and treatment of cardiovascular disease.

1. Introduction

Diseases of the vascular system remain the leading cause of mortality and morbidity in developed countries despite considerable therapeutic progress in recent years (Ku 1997, Berger and Jou, 2000). Thrombis formation can lead to various medical conditions including ischemia, atherosclerosis, and plaque rupture, the primary cause of stroke.

Much progress has been made over the last 50 years in our understanding of the mechanisms involved in the formation of arterial stenoses. The importance of flow properties on the growth of atherosclerotic legions was first speculated in the late 1950s and early 1960s due to the observation that certain sites in the vasculature show a predilection to sclerotic growth. While environmental factors (age, diet, stress, hypertension, cholesterol level) would be expected to act systematically, plaque growth preferentially occurs in regions where the vessel geometry will cause large changes in flow properties, specifically bifurcations and regions of high curvature (Texon, 1960).

It is now accepted that gradients in shear stress, both spatial and temporal, are the primary cause of atherogenesis (Berger and Jou, 2000). Shear stress plays a vital role in platelet activation and adhesion. Furthermore, subtle shear stress changes have been shown to modulate thrombus formation and plaque rupture. It follows therefore, that blood flow rate and velocity information are of critical importance for the diagnosis of vascular disease and methods to perform accurate and reliable assessment of instantaneous blood flow and velocity in a minimally or non-invasive manner are needed. A thorough understanding of the relationship between shear stress and atherosclerosis will aid developments in the diagnosis and treatment of cardiovascular disease. Shear stress may be calculated from direct velocity field measurements of high spatial resolution.

It is clear that there is a need to accurately characterise the velocity fields present in various physiologically relevent conditions, particularly in those regions prone to atherosclerosis. The flows present in these regions are pulsatile, highly three-dimensional and thus extremely difficult to measure accurately. Mechanical factors such as vessel compliance add another level of complexity to the flow. Along with the macroscopic mechanical aspects, cellular and sub-cellular level processes further complicate the system. These include platelet adhesion, cell transport dynamics and endothelial response to hemodynamic factors. The variety of factors influencing the flow properties are extremely difficult to replicate *in vitro,* hence the ability to measure blood flow fields *in vivo* is required. This necessitates measurement through opaque tissue. Venneman *et al.* (2006) identifies limitations of the currently available *in vivo* blood flow measurement techniques as the inability to measure internal flows at high temporal and spatial resolution, over the full range of scales from macroscopic to microscopic.

Various measurement techniques are in use or under development for the measurement of internal flow fields for cardiovascular research. These include magnetic resonance imaging (MRI) based velocimetry, ultrasound particle image velocimetry, and more recently X-ray particle image velocimetry.

Magnetic resonance velocimetry (MRV) has emerged as a viable non-invasive method capable of measuring three components of velocity in complex three-dimensional geometries. For technical details of MRI based flow measurement techniques and some examples the reader is referred to the recent review by Bonn *et al*. (2008). Limitations exist in MRI based velocimetry due to the fact that spatial resolution, temporal resolution, velocity resolution, signal to noise ratio (SNR), and scan time are all interdependent. For example, high spatial resolution scanning degrades temporal resolution and SNR (Taylor and Draney, 2004).

Ultrasound particle image velocimetry, also called echo PIV, combines ultrasound echo images with standard particle image velocimetry algorithms to measure velocity (Kim *et al.* 2004).

Ultrasound contrast agents (micro-bubbles) are used as seeding particles. The seeding particles reflect a scanned ultrasound beam, and the time between emission and detection of the beam is used to determine the depth of the echo. Liu *et al.* (2008) successfully measured flows in vitro in models of diseased vasculature. Echo PIV shows great potential for noninvasive *in vivo* blood flow measurement due to the ability to measure through opaque objects, however current techniques are severely limited in resolution, with the maximum spatial resolution achieved to date being 0.4 mm (Zheng *et al.* 2006).

X-ray particle image velocimetry (X-ray PIV) is emerging as a method for high resolution internal blood flow field measurement. The penetration achievable with X-rays makes this imaging mode ideal for *in vivo* blood flow field measurement. Recent advances in X-ray phase contrast imaging (PCI) provide the ability to differentiate soft tissue, which is not easily achieved using standard absorption based X-ray imaging (Paganin).

Probably the first study to combine X-ray imaging with particle velocimetry methods was published by Seeger *et al.* (2001). This study measured particle displacements in bubble columns using particle tracking. A medical biplane X-ray source was used to image the particles from orthogonal perspectives, allowing three components of velocity to be reconstructed. The measurements were severely limited in spatial and temporal resolution due to limitations in the imaging equipment and the low seeding density necessary to identify individual particles.

Lee and Kim combined synchrotron PCI and PIV techniques to measure flow in opaque tubes, both with particles (Lee and Kim, 2003), and red blood cells as tracers (Kim and Lee, 2006). These studies use standard planar PIV analysis on projected particle images. The methods described in these studies are therefore limited to two components of velocity within the two dimensional projected image plane.

Several recent studies have described X-ray PIV techniques for three dimensional flow field measurement. These methods all require assumptions to be made about the flow field to reconstruct three dimensional velocity fields using image pairs taken at a single projection angle.

Im *et al.* (2007) used particle tracking techniques to determine the velocity distribution within a tube. An axisymmetric computed tomographic reconstruction was then performed on this distribution data to reconstruct the three dimensional velocity field. This technique is necessarily limited in spatial resolution by the use of particle tracking. Additionally, the velocity reconstruction method used is only applicable to axisymmetric flows in axisymmetric geometries.

Fouras *et al.* (2007) developed a method for reconstruction of two component, three dimensional

velocity profiles from single projection images. The study showed that the cross-correlation functions calculated using X-ray projection images will be made up of contributions from each velocity present within the measurement volume, and are representative of the probability density function (PDF) of the flow field within the volume. Using this information in combination with certain assumptions about the flow allows the three dimensional velocity profile to be reconstructed. The technique is capable of three dimensional measurement, however requires *a priori* knowledge of the flow field and is therefore limited in its application.

Irvine *et al.* (2008) describes a method for the reconstruction of three dimensional flow fields using X-ray imaging and PIV methods. This technique uses an inverse Abel transform to reconstruct the three dimensional velocity field, using the velocity PDF calculated from cross-correlation analysis of interrogation regions. While the inverse Abel transform assumes axisymmetry, the technique is not limited in spatial resolution by particle tracking, as in Im *et al.* (2007). The use of phase contrast imaging in combination with phase retrieval in this technique enhances signal to noise ratio.

The aforementioned X-ray PIV techniques use single projection images, insufficient for evaluating three components of velocity. Images taken at a single projection angle contain no displacement information in the direction parallel to the X-ray beam. This limits single projection X-ray PIV to two component velocity measurements. Furthermore, no information regarding the velocity profile in the dimension perpendicular to the image plane is available, and therefore true three dimensional measurement is not possible without assumptions being made about the flow. The proposed technique uses multiple projection angles to overcome the limitations associated with single projection X-ray PIV. This allows true three component, three dimensional PIV measurement from two dimensional images.

2. Velocity Reconstruction Algorithm

Fig. 1 shows a schematic diagram of the X-ray illumination and imaging set up for X-Ray PIV. Unlike traditional PIV, which uses a thin laser sheet to illuminate the measurement region, an X-ray beam travels through a measurement volume and is projected onto a scintillator screen. The scintillator converts the X-rays to visible light, forming a two dimensional projection of the measurement volume. This projection is then captured using an optical imaging system. As in traditional PIV, images are discretised into interrogation regions. Each interrogation region contains particle displacement information from the entire measurement volume, projected onto a two-dimensional image plane. Fouras *et al.* (2007) showed that each velocity present within the measurement volume will contribute to the cross correlation function calculated from the X-ray projection image. Using this information the velocity PDF can be determined for each interrogation volume, and hence the velocity distribution can be reconstructed.

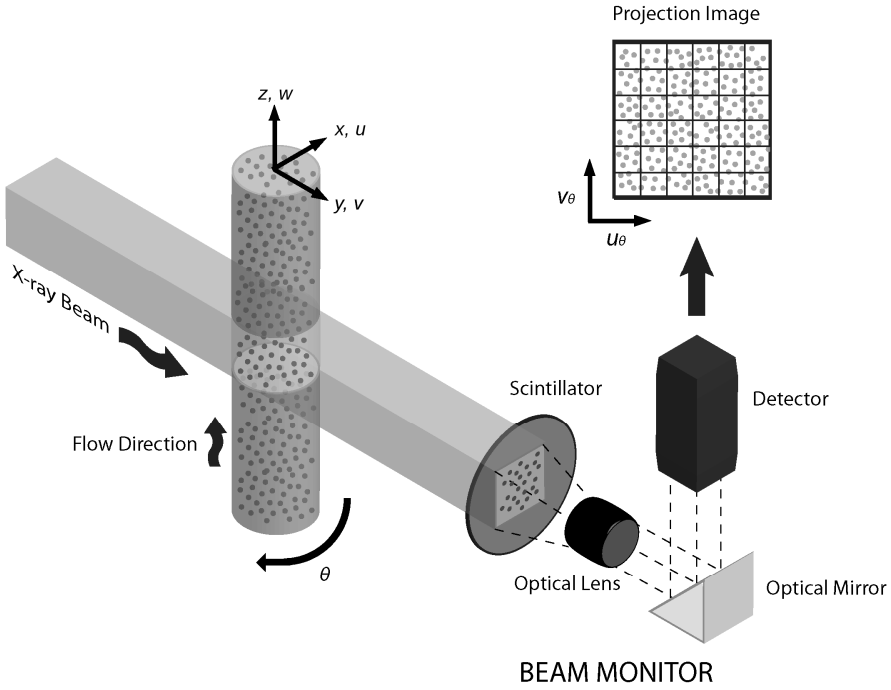

Fig. 1 Schematic of experimental setup for X-ray PIV. Particle projection images are acquired using a scintillator crystal and optical CCD detector system. Velocity coordinates *u, v* and *w* are fixed to the flow model and rotate with θ. Projected velocity coordinates u_θ and v_θ represent the horizontal and vertical components of velocity respectively for each θ on the projected image plane.

The velocity reconstruction algorithm is described in Fig. 2. The velocity field is reconstructed in axial slices, defined by the rows of interrogation regions for all projection angles. Fig. 1 defines the coordinate system. Velocity coordinates *u, v* and *w* are fixed to the flow model and rotate with θ. Projected velocity coordinates u_θ and v_θ represent the horizontal and vertical components of velocity respectively for each θ on the projected image plane.

Two dimensional cross correlation is performed on each interrogation region, for each projection, within a slice. Correlation ensemble averaging is used to reduce the effects of false particle correlations. For computational efficiency, the 2D correlation function is then projected into two, 1D correlation functions, representing the u_θ and v_θ velocity data. This is implemented by integration of the pixels in each column and row of the 2D correlation function, for u_θ and v_θ respectively. All subsequent procedures can then be performed in one dimension, for each velocity component individually, vastly reducing computer memory and processor demands

A three component, two dimensional, bicubic spline model represents the velocity profile for each slice. The three components of velocity (*u*, *v* and *w*) are defined at node points on a rectangular grid, and bicubic spline interpolation is used between points to define the velocity profile for each slice.

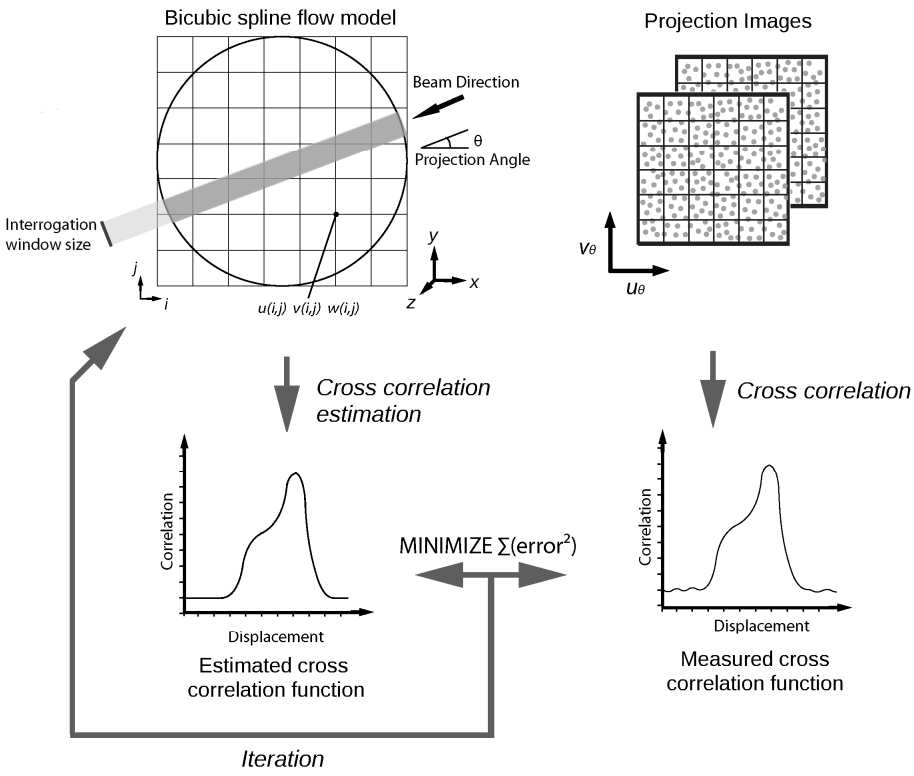

Fig. 2 Velocity reconstruction algorithm. The error between the estimated and measured cross correlation is minimized for all projections and measurements within a slice simultaneously, resulting in a model which accurately represents the velocity field.

Estimated cross-correlation functions are generated for every angle and every interrogation region within each slice. The PDF for each interrogation window, at each projection angle are constructed. These are calculated by integration of a section of the velocity model corresponding to the measurement volume imaged for each interrogation window, at each projection angle, for u_θ and v_θ individually. Values of w correspond directly to v_θ for all projection angles. The value of u_θ for each θ will be equal to the vector sum of u and v, projected onto a line given by the projection angle, according to Eq. (1).

$$u_\theta = v\cos(\theta) + u\sin(\theta) \tag{1}$$

The estimated cross-correlation functions are then generated using convolution of the measured auto-correlation function with the velocity probability density function for the interrogation region. The solution is implemented using a non-linear least squares iterative scheme. The velocity components at each node in the flow model are optimised to minimise the error between the measured and estimated cross-correlation functions, across all projection angles and interrogation regions simultaneously within a slice, resulting in a flow model which accurately represents the velocity profile within that slice. Combining the results from all slices within the measurement volume yields the three dimensional velocity field.

3. Results and Discussion

The technique was tested using synthetically generated particle projection image pairs. The velocity components *u(x,y), v(x,y),* and *w(x,y)* are defined by a two dimensional polynomial function describing the respective particle displacement between image frames, Δx, Δy, and Δz. Note that only a single slice was reconstructed. Two flow cases were chosen: an axisymmetric flow profile (parabolic in *w,* and diverging in *u* and *v)* (Fig. 4), and an asymmetric three component flow, reversing in *w* with cross flow (Fig. 5).

The functions used to define inter-frame particle displacement for the axisymmetric and asymmetric cases are shown in Eq. (2) and Eq. (3) respectively:

$$\begin{aligned} \Delta x(x,y) &= 10(y - x^2 y - y^3) \\ \Delta y(x,y) &= 10(x - xy^2 - x^3) \\ \Delta z(x,y) &= 30(1 - x^2 - y^2) \end{aligned} \tag{2}$$

$$\begin{aligned} \Delta x(x,y) &= 10(1 - x^2 - y^2) \\ \Delta y(x,y) &= 10(1 - x^2 - y^2) \\ \Delta z(x,y) &= 50(2x^3 - x^5 + xy^2 - y^2 x^3 - x) \end{aligned} \tag{3}$$

Synthetic projection images were generated for the two flow cases. A distribution of particles radii between 3 and 4 pixels was used, with a particle density of 8.90 x 10^{-6} particles / voxel. The reconstruction was performed using a bicubic spline flow model, based on a 7 x 7 rectangular grid, interpolated onto a 200 x 200 pixel sub-grid. Each pixel on the subgrid is included in the correlation estimations and contributes to the measured flow profile, resulting in a vector field of 200 x 200 measurements.

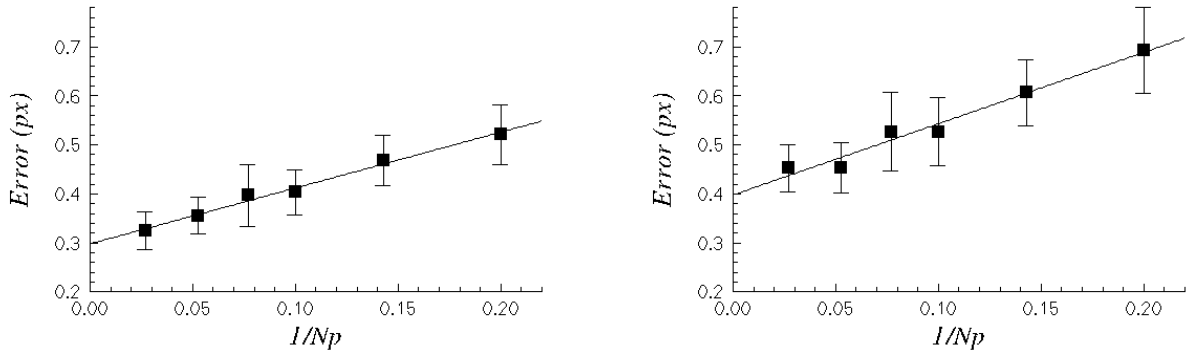

(a) (b)

Fig. 3 Relationship between RMS error and number of projection angles, for axisymmetric (a) and asymmetric (b) flow cases. Error bars show the standard deviation.

The relationship between the number of projection angles (N_p) and the velocity reconstruction accuracy was determined for both flow cases. Velocity reconstructions were performed for ten separate image sets, for 5, 7, 10, 13, 19 and 37 projection angles evenly spaced from 0 to 180 degrees (inclusive). Correlation functions for 10 image pairs were ensemble averaged to reduce the effect of false particle correlation. Fig. 3 shows the total RMS error plotted against $1/N_p$. As expected, the error is seen to decrease with an increasing number of projections. An RMS error is of less than 0.5 px was achieved with as few as 13 projections for the asymmetric case, and 7 projections for the axisymmetric case.

Fig.4 and Fig. 5 show the flow models used to generate the synthetic data, and velocity reconstructions for the two flow cases, using 19 projections, plotted as particle pixel displacement vs. location. The velocity reconstruction algorithm was able to accurately reconstruct the flow profiles in both cases. Fig. 6 shows the cross section of the *w* component of velocity, demonstrating the high level accuracy achieved.

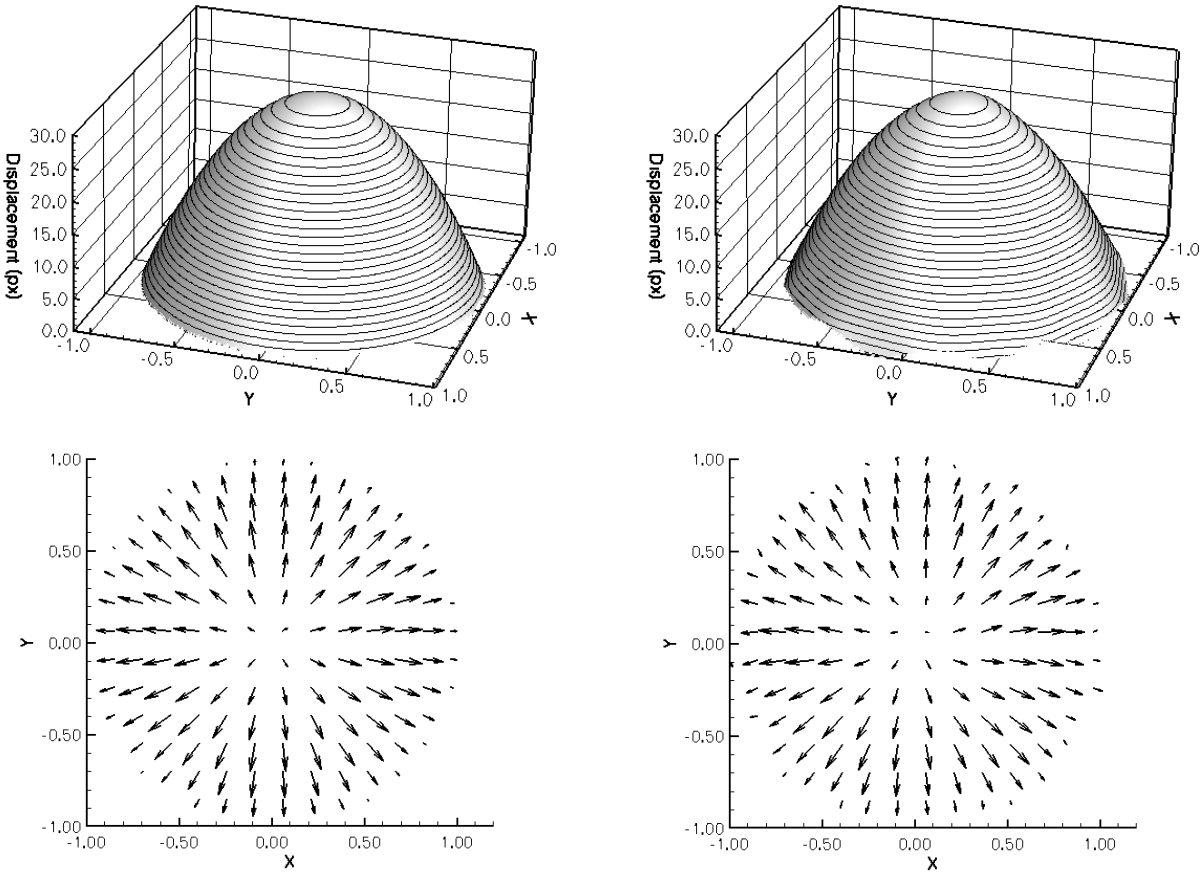

(a) (b)

Fig. 4 Flow field used to generate synthetic data (a) and velocity reconstruction result (b) for axisymmetric flow case, for Δw (top) and $\Delta u + \Delta v$ (bottom). Note that vector field is shown with reduced resolution for clarity. Actual measured vector field contains 200 x 200 measurement vectors.

The results demonstrate the technique's ability to accurately measure three components of velocity in complex flow fields, such as those which occur in the vasculature. The method offers a considerable improvement to previous X-ray PIV techniques, which are limited to two components of velocity measurement. The minimisation of X-ray dose is important for safe clinical application of this method. X-ray dose is directly proportional to the number of images acquired. It was found that the technique performs to within 0.5 px RMS error with as few as 13 projections and 10 ensemble averages, resulting in a total dose equivalent to around 130 images required for a single scan. This is less than half the typical dose for clinical computed tomographic (CT) scans, which generally require approximately 300 projection images

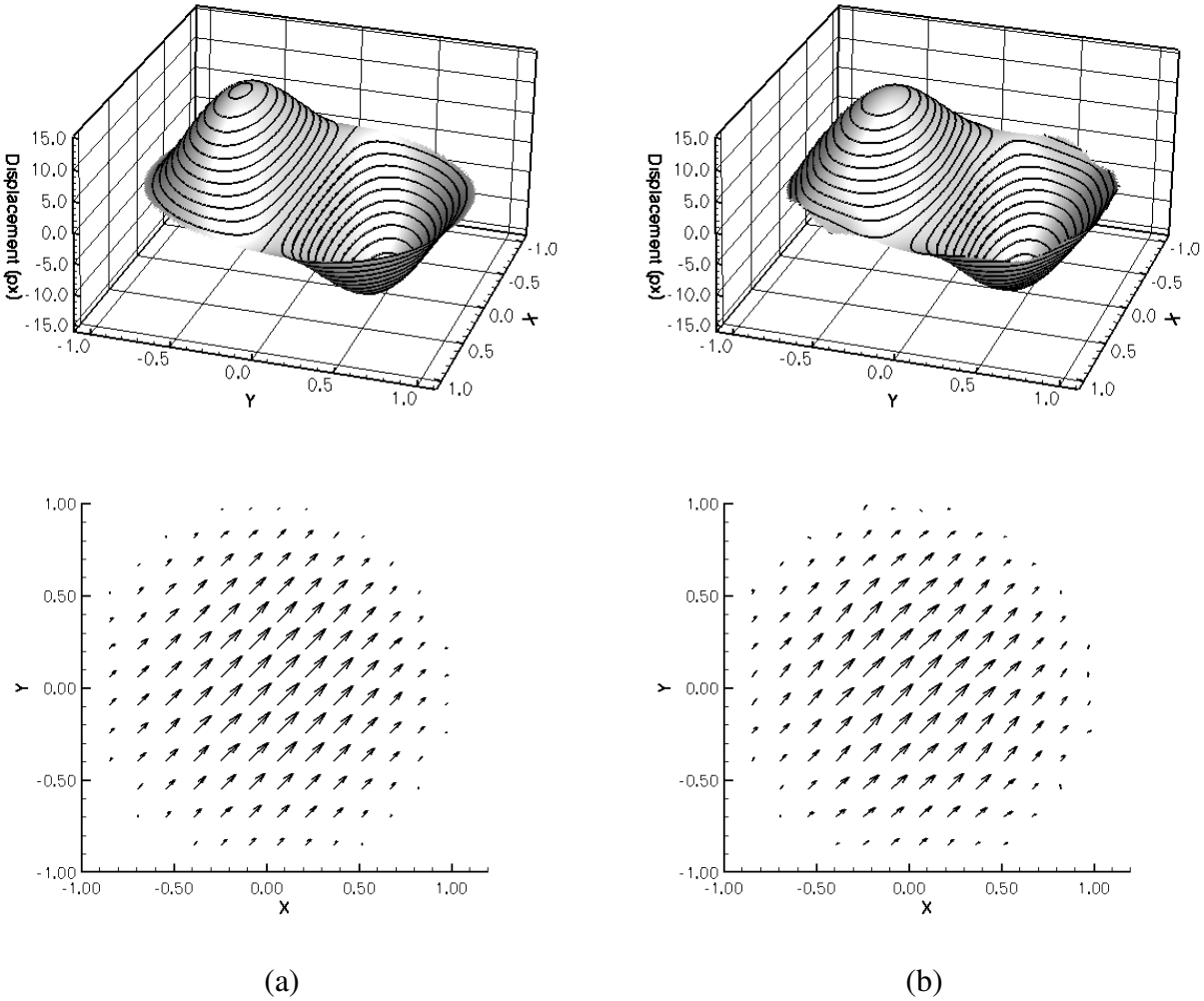

Fig. 5 Flow field used to generate synthetic data (a) and velocity reconstruction result (b) for asymmetric flow case, for Δw (top) and $\Delta u + \Delta v$ (bottom). Note that vector field is shown with reduced resolution for clarity. Actual measured vector field contains 200 x 200 measurement vectors.

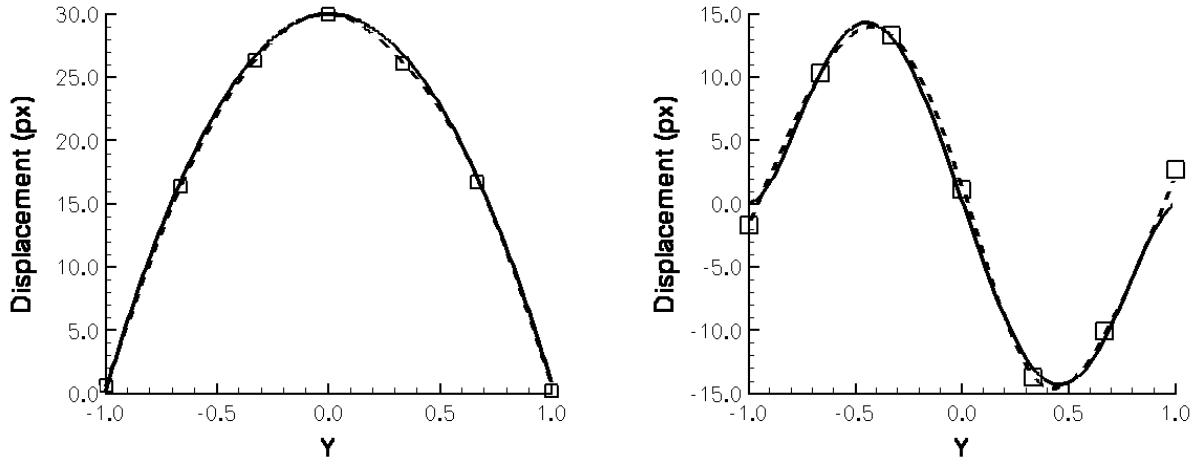

(a) (b)

Fig. 6 Cross section of velocity reconstruction results for axisymmetric (a) and asymmetric (b) flows showing exact solution (solid), reconstruction result (dashed) and flow model grid node values (squares).

4. Conclusions

The ability to measure complex blood flow fields *in vivo* with high resolution is an important capability in determining the effects of blood flow properties on the development of cardiovascular diseases such as atherosclerosis.

A method has been proposed for three dimensional, three component velocity measurements using X-ray PIV. Current single projection X-ray PIV techniques are limited to two components of measurement. The proposed method utilises multiple projection angles to overcome these limitations.

The technique was tested using synthetically generated particle projection images. Two case studies were used: a three component axisymmetric flow, and a three component asymmetric flow. The technique was able to resolve all three components of flow to a high degree of accuracy.

The effect of the number of projection angles on the accuracy of the velocity reconstruction technique was investigated. It was found that the technique performs well with as few as 13 projections and 10 ensemble averages. As X-ray dose must be carefully managed, the low number of images required for an accurate velocity reconstruction is important for the safe application of this technique in a clinical setting.

The proposed method represents a significant advancement in X-ray PIV techniques. The ability to measure complex three dimensional flow fields in internal vessels in a non-invasive manner has a wide variety of applications in cardiovascular research, and fluid mechanics. The use of this technique in a clinical setting will have a significant impact in the treatment and diagnosis of cardiovascular disease.

5. References

Berger SA, Jou LD. (2000) Flows in stenotic vessels. Ann Rev Fluid Mech 32: 347-382

Bonn d, Rodts S, Groenink M, Rafai S, Shahidzadeh-Bonn N, Coussot P (2008) Some applications of magnetic resonance imaging in fluid mechanics: Complex flows and complex fluids. Ann Rev Fluid Mech 40:209-233

Fouras A, Dusting J, Lewis R, Hourigan K (2007) Three-dimensional synchrotron X-ray particle image velocimetry. J App Phys 102 (6)

Im KS, Fezzaa K, Wang YJ, Liu X, Wang J, Lai MC. (2007) Particle tracking velocimetry using fast X-ray phase-contrast imaging. Appl Phys Lett 90(9)

Irvine SC, Paganin DM, Dubsky S, Lewis RA, Fouras A (2008) Phase retrieval for improved 3-D velocimetric analysis of X-ray blood flow speckIte patterns. Appl Phys Lett (Submitted for review)

Kim HB, Hertzberg JR, Shandas R (2004) Development and validation of echo PIV. Exp Fluids 36: 455-462

Kim GB, Lee SJ (2006) X-ray PIV measurements of blood flows without tracer particles. Exp Fluids 41: 195-200

Ku DN (1997) Blood flow in arteries. Ann Rev Fluid Mech 32: 347-382

Lee SK, Kim GB. (2003) X-ray particle image velocimetry for measuring quantitative flow information inside opaque objects. J Appl Phys 94(5): 3620 – 3623

Liu L, Zheng H, Williams L, Zhang F, Wang R, Hertzberg J, Shandas R (2008) Development of a custom-designed echo particle image velocimetry system for multi-component hemodynamic measurements: system characterisation and initial experimental results. Phys Med Biol 53:1397-1412

Paganin DM (2006) Coherent X-ray optics. Oxford University Press

Seeger A, Affeld K, Goubergrits L, Kertzscher U, Wellnhofer E (2001) X-ray based assessment of the three-dimensional velocity of the liquid phase in a bubble column. Exp Fluids 31:193-201

Taylor CA, Draney MT (2004) Experimental and computational methods in cardiovascular fluid mechanics. Ann Rev Fluid Mech 36:197-231

Texon, M (1960) The hemodynamic concept of atherosclerosis. The American Journal of Cardiology 5(3): 291 – 294

Venemann P, Lindken R, Westerweel J (2007) In vivo whole-field blood velocity measurement techniques. Exp Fluids 42:495-511

Zheng H, Liu L, Williams L, Hertzberg JR, Lanning C, Shandas R (2006) Real time multicomponent echo particle image velocimetry technique for opaque flow imaging Appl. Phys. Lett. 88:261,915(1)-261,915(3)